# MODULAR DRIVEN WHEELCHAIR BOND GRAPH MODELLING

**A. Fakri, J.P. Vilakazi**

*Université Paris-Est*
*ESIEE Paris*
*Département Systèmes Electroniques*
Cite Descartes
Bd Blaise Pascal – BP 99
93162 Noisy le Grand Cedex

[(a)]fakria@esiee.fr, [(b)] vilakazj@esiee.fr

**ABSTRACT**
Bond Graphs (BG) have become popular and are largely employed nowadays as efficient graphical description of multi-domain dynamic systems. This modelling technique is used in this paper to study the dynamics of an ordinary Manual Propelled wheelchair (MPW) and a mechatronic drive module (MDM). This electric powered mechatronic drive module is hence linked to the ordinary MPW system to obtain a modular driven manual wheelchair (MDMW). The Bond Graphs of these systems are constructed and mathematical models extracted in terms of state space differential equations. Simulation results illustrating the behaviour of some dynamic variables are also shown. This paper is aimed at providing good support for the academic field on dynamic system modelling using Bond Graph and Matlab Simulink.

Keywords**:** dynamic system, Bond Graph, modelling tools, test bed structure

## 1. INTRODUCTION

Improving the lives of the mobility impaired people has always been every states focus (wheelchairnet.org). The investigation on improving specifically the ordinary MPW propulsion method (which results in upper extreme injuries on long term users) has become increasingly imperative due to the growing population of the manual wheelchair users and the requirements for efficient mobility to maintain a quality of live equivalent to the general population**.**

The motivation for this work derives from attempts to employ few portable mechatronic drive modules which can be coupled when necessary to a large scale of MPW systems with the aims of improving propulsion efficiency. The engagement of such a module on MPW is illustrated on Figure 1. This yields good advantage to the system since the weight of the module is imposed on the module itself, thus prevents deformation of the structure. In the next, the modelling of such a system is presented in terms of Bond Graphs.

Currently the subject of mechatronic system design has taken a new dimension since many researchers have turned their attention to emerging technologies that allows engineers to understand multidisciplinary systems. When creating a physical device, one of the major tasks is the implementation of the model which integrates the control system, sensors and actuators dynamics in order to allow the simulation software tools to be integrated in the modelling process. The bond graph methodology is a very well suited graphical tool for modular modelling approach based on energy transfer in multi-domain systems (Karnopp, Margolis and Rosenberg 2006). We assume that the reader has some knowledge on the BG modelling method employed; therefore a brief review is given below.

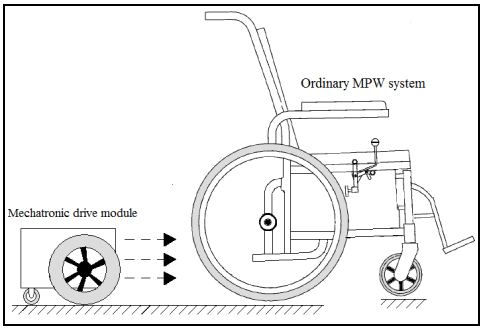


Figure 1: Manual Propelled Wheelchair (MPW) System with the Mechatronic Module

BGs represent the elementary transfer and storage of energy through different dynamic component on the system, the 0 and 1 junction are used to denote common effort and flow cases, thus permitting the extraction of balance junction dynamic equations which in turn enables derivation of mathematical models of the system. Each graphical bond carries power which is product of two variables flow and effort. Power is transferred between different domains with the use of *gyrator* and *transformer* elements. For control purposes, source of *flow* or *effort* is used as input to the system. Some part of the transferred energy is dissipated in resistive elements, Bond Graphically denoted by symbol *(R)* or stored in kinetic or potential form in respectively inertial *(I)* or capacitive (C) elements. For more information, readers may refer to (Karnopp, Margolis and Rosenberg 2006).

If properly applied, the bond graph methodology enables one to develop a graphical model that is consistent with the first principle of energy conservation without having the need to start with establishing and

reformulating equations. (Dauphin-tanguy 2000). The studied systems test bed structures are analysed and model components elaborated. Mathematical models (in terms of state space differential equations) and simulation results of these systems are also presented. In the next section, we present the decomposition of the MPW, its BG model, State space model and simulation results in an obstacle avoidance predetermined trajectory. Note that the simulation was carried out on Matlab Simulink using the BG equivalent block diagram constructed directly from the BG model; this method is presented in (Fakri, Rocaries and Carriere 1997). Section 3, presents the schematic of the mechatronic drive module, its BG model as well as simulation results in a predetermined trajectory showing behaviour of this system in open and close-loop control. Section 4 presents the whole system (MDM coupled on MPW) BG model and simulation in the same trajectory. The last section gives some conclusion and future work.

## 2. MANUAL PROPELLED WHEELCHAIR

### 2.1. Description and test bed

MPW is required in hospitals and old age institutions to transport patients who are too unwell to walk (Abel and Frank 1991).The user can manoeuvre the chair by turning the hand push rims attached to the rear wheels, as shown in Figure 1. For users who cannot operate the MPW, handles are made available for assistance from an attendant.

An illustration of an ordinary MPW test bed structure used in this modelisation is depicted on Figure 2. It essentially consists of two caster and manual rear wheels. An approach of a two wheel drive robotic system described in (Klancar, Zupancic and Karba 2007) has been applied in this modelling with the caster wheels lumped together and assumed to be imposing resistive force to the systems flow. $V_{CG}$ and $\omega_{CG}$ represents the centre of mass velocity and inertial mass rotation, $\omega_l$ and $\omega_r$ indicates the angular velocity of the left and right wheels respectively, rear manual wheel radius and wheelchair width are represented by (***r)*** and *(Lw)* respectively. Parameter values are given in the Table. The below matrices (1) shows the kinematic mathematical model of the system, where: $\theta$ is the orientation angle, $x$ and $y$ shows the systems geometric position respectively:

$$\begin{bmatrix} x \\ y \\ \theta \end{bmatrix} = r \begin{bmatrix} \frac{\cos\theta}{2} & \frac{\cos\theta}{2} \\ \frac{\sin\theta}{2} & \frac{\sin\theta}{2} \\ \frac{2}{Lw} & \frac{-2}{Lw} \end{bmatrix} \begin{bmatrix} \omega r \\ \omega l \end{bmatrix} \quad (1)$$

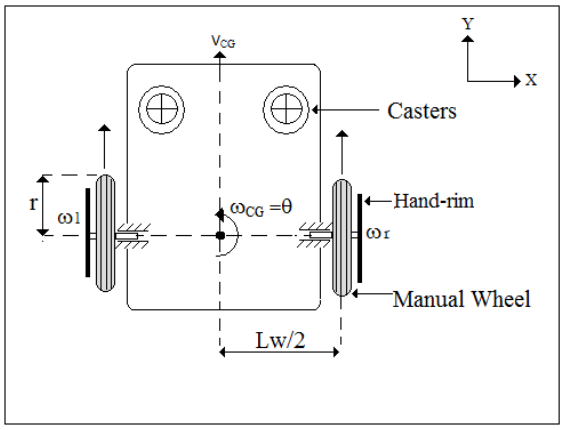


Figure 2: Top view of Manual Propelled Wheelchair (MPW) System

### 2.2. Bong Graph model of MPW

A remarkable feature of BGs is that an inspection of causal path can reveal information about structural control of the system behaviour. The survey of BG capabilities shows how this modelling technique serves as a core model representation, from which different information can be derived depending on purpose of the study (Gawthrop and Bevan 2007).

The test bed shown in Figure 2 is hence represented in an integral causalled BG shown in Figure 3. Where: *MSE:*$\tau$ [Nm] shows the source of effort generated from the tangential force applied by the user on the wheels, *L* [left] or *R* [right], *Jw_L* [kgm$^2$] is the rotational inertia of the rear wheels, *Rg* is the rear wheel to ground frictional constant, *Mt* [kg] is the total mass of the system, *Jt* [kgm$^2$] is the total inertial moment of the system, *Rc* is the losses on caster wheels during motion, *Rwc, Cwc* shows the wheel to structure coupling stiffness and elasticity respectively whilst *Cw and Rw* represents the rear wheels spring/damper spokes constants respectively. The non-linear *MTF* represents the energy transferred to structure depending on the applied force.

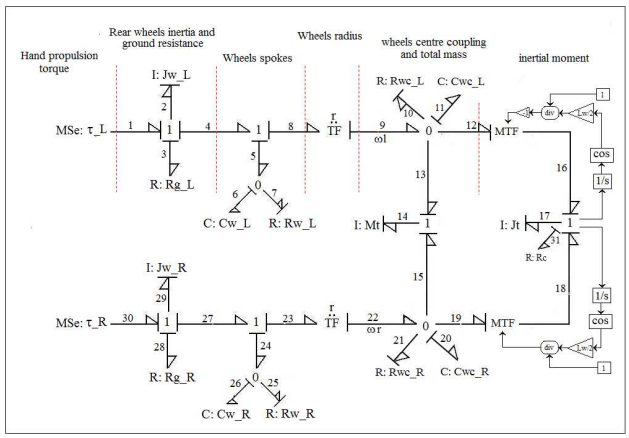


Figure 3: A Bond Graph representation of the MPW system

### 2.3. State Space Representation

The state space equations used by control engineers for system analysis and simulations (Klancar, Zupancic and Karba 2007; Gawthrop and Bevan 2007) are extracted directly from Figure 3. These can be used for controllability, observability and stability studies of the system. Computer software like CAMP-G, 20sim and Symbols can be used to extract these equations automatically. Equations 2 and 3 show the state space representation of MPW where *x*, *u* and *y* are the system state, input and output respectively. These equations are directly derived from the BG model in Figure 3.

$$\dot{x} = [\mathrm{A}]x + [\mathrm{B}]\mu \qquad (2)$$

$$\begin{bmatrix} e_2 \\ f_6 \\ f_{11} \\ e_{14} \\ e_{17} \\ f_{20} \\ f_{25} \\ e_{29} \end{bmatrix} = \begin{bmatrix} \dot{p}_2 \\ \dot{q}_6 \\ \dot{q}_{11} \\ \dot{p}_{14} \\ \dot{p}_{17} \\ \dot{q}_{20} \\ \dot{q}_{25} \\ \dot{p}_{29} \end{bmatrix} = [\mathrm{A}] \begin{bmatrix} p_2 \\ q_6 \\ q_{11} \\ p_{14} \\ p_{17} \\ q_{20} \\ q_{25} \\ p_{29} \end{bmatrix} + \begin{bmatrix} 1 & 0 \\ 0 & 0 \\ 0 & 0 \\ 0 & 0 \\ 0 & 0 \\ 0 & 0 \\ 0 & 0 \\ 0 & 1 \end{bmatrix} \begin{bmatrix} \tau L \\ \tau L \end{bmatrix}$$

Where:

$$\mathrm{A}=\begin{bmatrix} \frac{-Rg\_L}{JW\_L} & \frac{-1}{Cw\_L} & \frac{-k1}{Cwc\_L} & 0 & 0 & 0 & 0 & 0 \\ \frac{1}{JW\_L} & \frac{-1}{Rw\_LCw\_L} & 0 & 0 & 0 & 0 & 0 & 0 \\ \frac{k1}{JW\_L} & 0 & \frac{-Rwc\_L}{Cwc\_L} & \frac{-1}{Mt} & \frac{-1}{k2Jt} & 0 & 0 & 0 \\ 0 & 0 & \frac{1}{Cwc\_L} & 0 & 0 & \frac{1}{Cwc\_R} & 0 & 0 \\ 0 & 0 & \frac{-k2}{Cwc\_L} & 0 & 0 & \frac{1}{k3Cwc\_R} & 0 & 0 \\ 0 & 0 & 0 & \frac{-1}{Mt} & \frac{-1}{k3Jt} & \frac{-1}{Rwc\_RCwc\_R} & 0 & \frac{-k4}{Mt} \\ 0 & 0 & 0 & 0 & 0 & 0 & \frac{-1}{Rw\_RCw\_R} & \frac{1}{JW\_R} \\ 0 & 0 & 0 & 0 & 0 & \frac{-k4}{Cwc\_R} & \frac{-1}{Cw\_R} & \frac{-Rg\_R}{JW\_R} \end{bmatrix}$$

$$y = [C]\,x \qquad (3)$$

$$\begin{bmatrix} \omega_L \\ \omega R \\ VCG \\ \theta CG \end{bmatrix} = \begin{bmatrix} f_4 \\ f_{27} \\ f_{14} \\ f_{17} \end{bmatrix} = \begin{bmatrix} \frac{1}{Jw\_L} & 0 & 0 & 0 \\ 0 & \frac{1}{Jw\_R} & 0 & 0 \\ 0 & 0 & \frac{1}{Mt} & 0 \\ 0 & 0 & 0 & \frac{1}{Jt} \end{bmatrix} \begin{bmatrix} p_2 \\ p_{29} \\ p_{14} \\ p_{17} \end{bmatrix}$$

### 2.4. Simulation results

The general characteristics of the forces applied to the handrim during propulsion is sinusoidal and includes rapid rate of loading in the beginning of the push leading to an impact spike and followed by more gradual application and release of force. For the purpose of this study, the system was simulated with step input signals (representing the manual torque) to produce an obstacle avoidance predetermined trajectory.

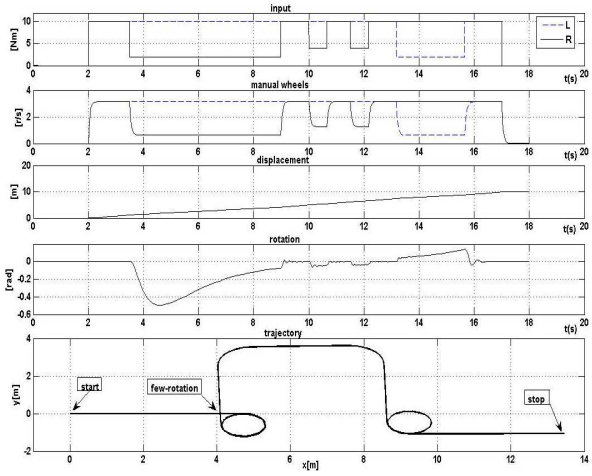


Figure 4: Manual Propelled Wheelchair Simulation Results

The main objective was to illustrate the behaviour of the MPW system without the MDM engaged on it. A combination of step signals in the range of 4 to 10Nm was applied on both wheels as depicted on Figure 4, position and orientation (with reference to the x-axis) were observed.

## 3. MECHATRONIC DRIVE MODULE

### 3.1. Description and Schematic

A typical mechatronic drive module (MDM) is depicted in Figure 5. It comprises of a direct current (DC) motor converting electric energy (from batteries in this case) into mechanical energy. Velocity reduction mechanical gears are used and the manner in which motorised wheels are coupled to the system is illustrated.

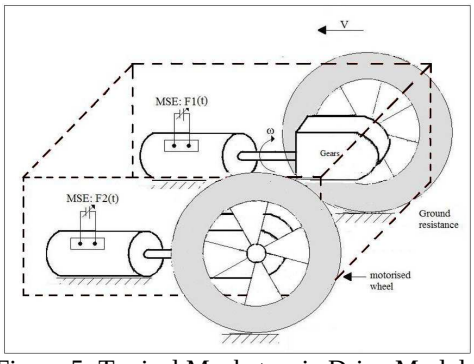


Figure 5: Typical Mechatronic Drive Module

The small values of rotational dampers and torsion springs on the shafts have been lumped together and represented by *Rs* and *Cs* respectively. This is a typical drive unit of an EPPW system.

### 3.2. Bond Graph model of MDM

Different components forming part of the MDM depicted on figure 5 are hence represented bond graphically in figure 6. This BG model is decomposed into four main parts, the first two representing the electric motor and the transmission gear, while the second shows the wheels inertia and the last showing the dynamics of the wheelchair structure built around the translational *Mt* and rotational *Jt* inertia. To study the dynamics of the system, the imperative outputs to be observed are $i_2$, $\omega_4$, $\omega_{13}$ and $v_{23}$ which denote the motor electric current, armature angular velocity, wheel angular velocity and the module lateral velocity or centre of mass respectively. The given state space differential equations further denotes all the outputs observed in this modelisation.

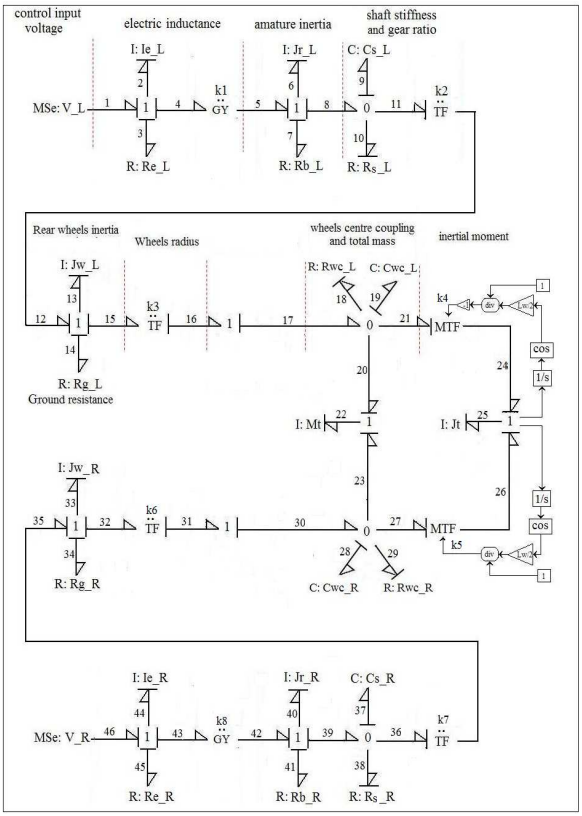


Figure 6: Bond Graph representation of MDM

### 3.3. State Space Representation

The equations 4 and 5 represent the state space models of the MDM system. These equations can be used for simulation, however in complex multidomain systems, the order increases and the difficulty of manual extractions of state spaces increases in proportion. This clearly denotes the difference between the Bond Graph and state space mathematical modelling.

$$\dot{x} = [A]x + [B]\mu \qquad (4)$$

$$\begin{bmatrix} e_2 \\ e_6 \\ f_9 \\ e_{13} \\ f_{19} \\ e_{22} \\ e_{25} \\ f_{28} \\ e_{33} \\ f_{37} \\ e_{40} \\ e_{44} \end{bmatrix} = \begin{bmatrix} \dot{p}_2 \\ \dot{p}_6 \\ \dot{q}_9 \\ \dot{p}_{13} \\ \dot{q}_{19} \\ \dot{p}_{22} \\ \dot{p}_{25} \\ \dot{q}_{28} \\ \dot{p}_{33} \\ \dot{q}_{37} \\ \dot{p}_{40} \\ \dot{p}_{44} \end{bmatrix} = [A] \begin{bmatrix} p_2 \\ p_6 \\ q_9 \\ p_{13} \\ q_{19} \\ p_{22} \\ p_{25} \\ q_{28} \\ p_{33} \\ q_{37} \\ p_{40} \\ p_{44} \end{bmatrix} + \begin{bmatrix} 1 & 0 \\ 0 & 0 \\ 0 & 0 \\ 0 & 0 \\ 0 & 0 \\ 0 & 0 \\ 0 & 0 \\ 0 & 0 \\ 0 & 0 \\ 0 & 0 \\ 0 & 0 \\ 0 & 1 \end{bmatrix} \begin{bmatrix} VL \\ VR \end{bmatrix}$$

Where:

$$A = \begin{bmatrix} \frac{-R_{e\_L}}{Ie\_L} & \frac{-k_1}{Jr\_L} & 0 & 0 & 0 & 0 & 0 & 0 & 0 & 0 & 0 & 0 \\ \frac{k_1}{Ie\_L} & \frac{-R_{b\_L}}{Jr\_L} & \frac{-1}{Cs\_L} & 0 & 0 & 0 & 0 & 0 & 0 & 0 & 0 & 0 \\ 0 & \frac{-1}{Jr\_L} & \frac{-1}{R_{g\_L}Cs\_L} & \frac{-1}{k_2Jw\_L} & 0 & 0 & 0 & 0 & 0 & 0 & 0 & 0 \\ 0 & 0 & \frac{1}{k_2Cs\_L} & \frac{-R_{g\_L}}{Jw\_L} & \frac{-k_3}{Cwc\_L} & 0 & 0 & 0 & 0 & 0 & 0 & 0 \\ 0 & 0 & 0 & \frac{k_3}{Jw\_L} & \frac{-1}{R_{wc\_L}Cwc\_L} & \frac{-1}{Mt} & \frac{k_4}{Jt} & 0 & 0 & 0 & 0 & 0 \\ 0 & 0 & 0 & 0 & \frac{1}{Cwc\_L} & 0 & 0 & 0 & \frac{1}{Cwc\_R} & 0 & 0 & 0 \\ 0 & 0 & 0 & 0 & \frac{k_4}{Cwc\_L} & 0 & 0 & \frac{1}{k_5Cwc\_R} & 0 & 0 & 0 & 0 \\ 0 & 0 & 0 & 0 & 0 & \frac{-1}{Mt} & \frac{-1}{k_5Jt} & \frac{-1}{R_{wc\_R}Cwc\_R} & \frac{k_6}{Jw\_R} & 0 & 0 & 0 \\ 0 & 0 & 0 & 0 & 0 & 0 & \frac{-k_{26}}{Cwc\_R} & \frac{-R_{g\_R}}{Jw\_R} & \frac{1}{k_7Cs\_R} & 0 & 0 & \\ 0 & 0 & 0 & 0 & 0 & 0 & 0 & \frac{-1}{k_7Jw\_R} & \frac{-1}{R_{g\_R}Cs\_R} & \frac{-1}{Jr\_R} & 0 & \\ 0 & 0 & 0 & 0 & 0 & 0 & 0 & 0 & \frac{-1}{Cs\_R} & \frac{-R_{b\_R}}{Jr\_R} & \frac{k_8}{Ie\_R} & \\ 0 & 0 & 0 & 0 & 0 & 0 & 0 & 0 & 0 & \frac{-k_8}{Jr\_R} & \frac{-R_{e\_R}}{Ie\_R} & \end{bmatrix}$$

$$y = [C]\,x \qquad (5)$$

$$\begin{bmatrix} iL \\ \tau L \\ \omega mL \\ \omega wL \\ VCG \\ \theta CG \\ \omega wR \\ \omega mR \\ \tau R \\ iR \end{bmatrix} = \begin{bmatrix} i_2 \\ e_6 \\ f_8 \\ f_{13} \\ f_{22} \\ f_{25} \\ f_{33} \\ f_{39} \\ e_{40} \\ i_{44} \end{bmatrix} = \begin{bmatrix} \frac{1}{Ie\_L} & 0 & 0 & 0 & 0 & 0 & 0 & 0 \\ \frac{k1}{Jr\_L} & 0 & 0 & 0 & 0 & 0 & 0 & 0 \\ 0 & \frac{1}{Jr\_L} & 0 & 0 & 0 & 0 & 0 & 0 \\ 0 & 0 & \frac{1}{Jw\_L} & 0 & 0 & 0 & 0 & 0 \\ 0 & 0 & 0 & \frac{1}{Mt} & 0 & 0 & 0 & 0 \\ 0 & 0 & 0 & 0 & \frac{1}{Jt} & 0 & 0 & 0 \\ 0 & 0 & 0 & 0 & 0 & \frac{1}{Jw\_R} & 0 & 0 \\ 0 & 0 & 0 & 0 & 0 & 0 & \frac{1}{Jr\_R} & 0 \\ 0 & 0 & 0 & 0 & 0 & 0 & 0 & \frac{k8}{Jr\_R} \\ 0 & 0 & 0 & 0 & 0 & 0 & 0 & \frac{1}{Ie\_R} \end{bmatrix} \begin{bmatrix} p_2 \\ p_6 \\ p_{13} \\ p_{22} \\ p_{25} \\ p_{33} \\ p_{40} \\ p_{44} \end{bmatrix}$$

### 3.4. Simulation

Illustrated in figure 7 are some of the system outputs observed during motion in a space of 20x10m$^2$. The system was simulated for 45s with a profile of step input signals applied on the electric motor terminals ranging from 0 to24V, with maximum value resulting into a lateral velocity of 1.8m/s, and eventually brought to stationery position at t=36.

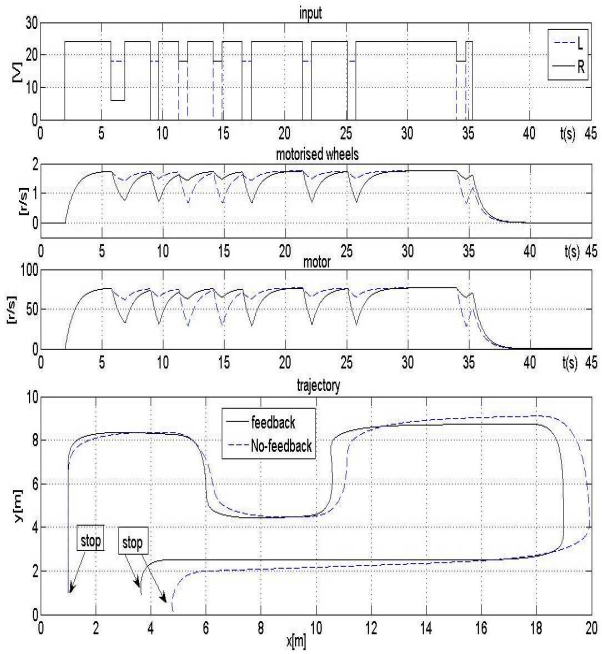


Figure 7: Mechatronic drive module simulation results

In all the graphs, the solid and dashed lines show the right and left side dynamics respectively. We can visualise that angular speeds of both the motors and wheels, follow the input profile. Rotation at the centre of mass was observed by an altering "rotation" signal (not shown). The predetermined trajectory is depicted on the lower graph with the system operating in both open and closed-loop control.

## 4. MODULAR DRIVEN MANUAL WHEELCHAIR

### 4.1. Test bed description

Ultimately, illustrated on figure 8 is the top view of an MDMW system model. The module introduces two more wheels on the existing four wheels of MPW. The module is assumed to be coupled on the same axes with the rear manual wheels as show below. *Lw/2* represents the width of MPW from centre of rotation to the centre of rear wheel. The BG and some simulations are shown in the next sections

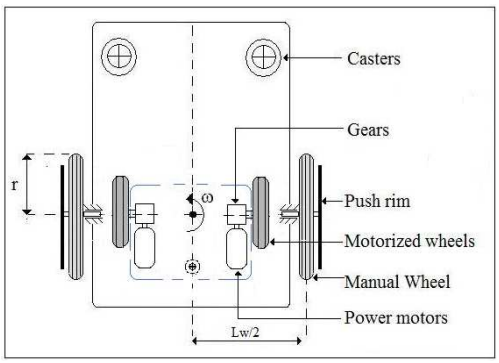


Figure 8: MDMW system

### 4.2. Bong Graph model

Bond graphs are based on energy exchange, and Figure 9 gives an illustration on how energy is transferred and exchanged from the voltage inputs to the MPW structure. This allows observation of different dynamic information and the system behaviour. The kinetic energy generated by the module is transmitted mechanically to the MPW system. In figure 9, the parameters *Mt and Jt* represent the translational and rotational inertia of the entire systems.

With the MDM serving as source of kinetic energy to the wheelchair system, the manual wheels of the MPW are now considered as passive. This introduces the unpreffered *derivative causality* at the manual wheels rotational inertia. The motorised and manual wheels angular velocities are observed. The following section gives the results obtained.

### 4.3. Simulation results

In order to observe and compare whether the MDM propels the MPW successfully, we used the same predetermined trajectory and profile of step input voltage signals (used on MDM) to the combined system. The results obtained are shown in figure 10. With more weight on the MDMW and operated in open loop control, the system displaced for 15m in 45sec instead of 32m.

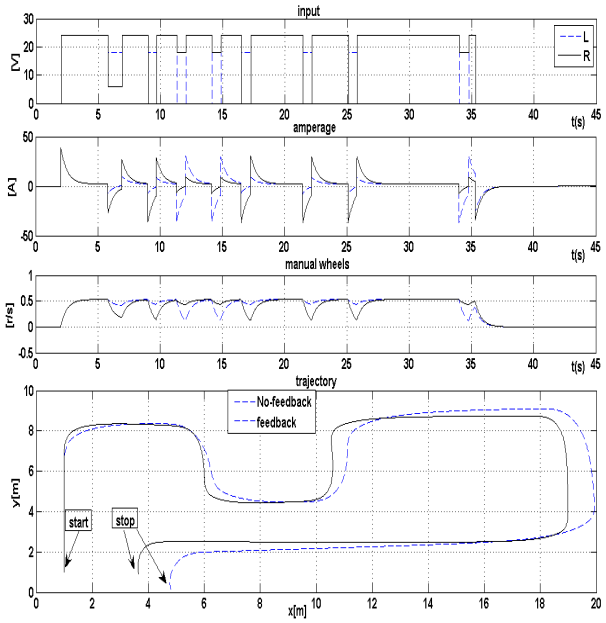


Figure 10: Modular Driven Manual Wheelchair simulation results

A local feedback from the motor's angular velocity including the PI controller was employed. Coupling stiffness increased. The system reaching the predetermined trajectory in the exact time; however more amperage consumption was noticed due to high propulsion torque required to withstand the increased translational inertia.

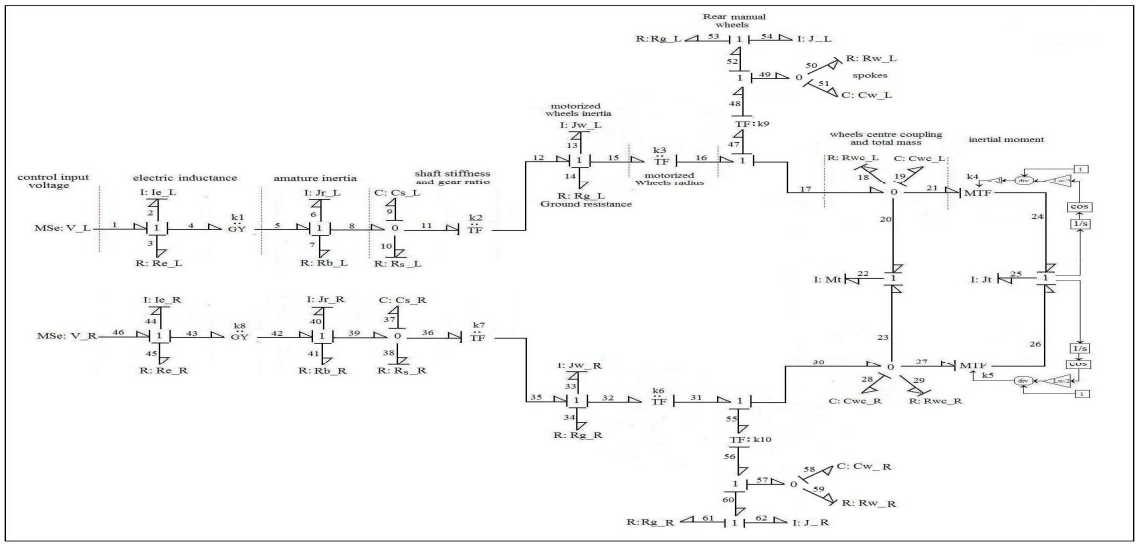


Figure 9: MDM attached to the MPW system

## 5. CONCLUSION AND FURTHER STUDIES

In this paper we have presented the Bond Graph modelling, analysis and simulation work of a mechatronic drive module and its coupling to the ordinary manual propelled wheelchair. The method was employed to study the different substructures and the linked systems. The models were simulated on a realistic area and can be used as a tutorial for the Bond graph studies of mobile systems.

In the near future, we will extend this work to the study of a battery and the charging system. These models will be utilised to design and implement real-time controller that can be implemented on digital control loops. We also plan to build a prototype that will be used to test the reliability functioning and to improve power efficiency management of this system.

Table: System Parameters

| Parameter | Description | Value |
|---|---|---|
| *Manual Propelled Wheelchair (MPW)* | | |
| MSe:τ | rear wheel propulsion torque (*Nm*) | *12* |
| Jw | rear wheel rotational inertia(*kgm²*) | *0.005* |
| Mt | systems mass *(kg)* | *100* |
| Jt | systems inertial moment *(kgm²)* | *64* |
| Rg | wheel to ground resistance | *0.006* |
| Cw | wheel spoke spring | *0.0021* |
| Rw | wheel spoke damper | *12* |
| r | rear wheel radius*(m)* | *0.30226* |
| Lw | wheelchair width*(m)* | *0.8* |
| *Mechatronic Drive Module (MDM)* | | |
| Ie | electric motor inductance *(H)* | *0.0033* |
| Re | electric motor resistance *(Ω)* | *0.9* |
| Jr | rotor rotational inertia*(kgm²)* | *0.078* |
| Rb | motor bearing damper*(Nm-s/rad)* | *0.008* |
| Mt | module mass*(kg)* | *30* |
| Jt | module inertial moment*(kgm²)* | *7.5* |
| Lw | module width*(m)* | *0.6* |
| Cs | motor to gear shaft torsion*(Nm/rad)* | *0.00237* |
| Rs | motor to gear shaft damper | *11* |
| $k_1$, $k_8$ | motor torque constant*(Nm/A)* | *0.288* |
| $k_2$, $k_7$ | mechanical gear ration | *0.18* |
| $k_3$, $k_6$ | motorized wheels radius*(m)* | *0.127* |
| MSe:L | control input voltage*(V)* | *24* |
| *Modular Driven Manual Wheelchair (MDMW)* | | |
| J | manual wheels *(kgm²)* | *0.005* |
| $K_9$, $k_{10}$ | manual wheels radius*(m)* | *0.30226* |
| Mt | combined systems total mass*(kg)* | *130* |
| Jt | total inertial moment*(kgm²)* | *83.5* |

## REFERENCES


Wheelchairnet.org, Discussion preparation for manual wheelchair propulsion. *Rehabilitation Engineering research Centre on Technology Transfer Federal Laboratory Consortium*: Mid Atlantic Region. http://www.wheelchairnet.org/ [15-04-2010].

Karnopp, D.C., Margolis, D.L., Rosenberg, R.C., 2006. *System dynamics: A Unified Approach 4th edition*. Wiley Publications.

Dauphin-Tanguy, G., 2000. *Les Bond Graphs*. Hermes edition .

Fakri, A., Rocaries, F., Carriere, A., 1997. A Simple method for the conversion of bond graph models in presentation by block diagrams. *International Conference on Bond Graph Modelling and Simulatio*, pp15-19. *ICBGM'97*. Phoenix Arizona.

Abel, E.N., Frank, T.G., 1991. *The design of an attendant propelled wheelchair*. prosthetic and orthotic inserthond.

Klancar, B., Zupancic, R., Karba, R., 2007. *Modelling and simulation of a group of mobile Robots*. Faculty of Electrical Engineering, University of Ljubljana, 1000 Ljubljana. Slovenia.

Gawthrop, P.J., Bevan, G.P., 2007. *TA Tutorial Introduction for Control Engineers. Bond Graph modeling*. IEEE Control Magazine, 24-45.